Preparation and Antibacterial Effects of PVA-PVP Hydrogels Containing Silver Nanoparticles

Haijun Yu,[1,2] Xiaoyi Xu,[1,2] Xuesi Chen,[1] Tiancheng Lu,[1,2] Peibiao Zhang,[1] Xiabin Jing[1]

[1]*State Key Laboratory of Polymer Physics and Chemistry, Changchun Institute of Applied Chemistry, Chinese Academy of Sciences, Changchun 130022, People's Republic of China*
[2]*Graduate School of Chinese Academy of Sciences, Beijing 100039, People's Republic of China*

Received 20 April 2006; accepted 14 May 2006
DOI 10.1002/app.24835
Published online in Wiley InterScience (www.interscience.wiley.com).

ABSTRACT: The poly(vinyl alcohol)/poly(*N*-vinyl pyrrolidone) (PVA–PVP) hydrogels containing silver nanoparticles were prepared by repeated freezing–thawing treatment. The silver content in the solid composition was in the range of 0.1–1.0 wt %, the silver particle size was from 20 to 100 nm, and the weight ratio of PVA to PVP was 70 : 30. The influence of silver nanoparticles on the properties of PVA–PVP matrix was investigated by differential scanning calorimeter, infrared spectroscopy and UV–vis spectroscopy, using PVA–PVP films containing silver particles as a model. The morphology of freeze-dried PVA–PVP hydrogel matrix and dispersion of the silver nanoparticles in the matrix was examined by scanning electron microscopy. It was found that a three-dimensional structure was formed during the process of freezing–thawing treatment and no serious aggregation of the silver nanoparticles occurred. Water absorption properties, release of silver ions from the hydrogels and the antibacterial effects of the hydrogels against *Escherichia coli* and *Staphylococcus aureus* were examined too. It was proved that the nanosilver-containing hydrogels had an excellent antibacterial ability. © 2006 Wiley Periodicals, Inc. J Appl Polym Sci 103: 125–133, 2007

Key words: silver; hydrogel; antibiotic; wound dressing

INTRODUCTION

Despite major advances in burn wound management and other supportive care regimens, infection remains the leading cause of morbidity in the thermally injured patients, and the search for different treatments and new ideas is continuing.[1] Silver metal and silver ions have been known as effective antimicrobial agents for a long time, The application of silver-binding membranes has recently been suggested to further reduce the silver toxicity, to retard the movement of silver ions, and to minimize silver absorption at a healing wound.[2–4]

There have been several kinds of silver-containing materials that can be used for wound dressing. For example, silver sulfadiazine containing chitosan-based wound dressing,[5–7] dendrimer–silver complexes and nanocomposites,[8] nanosilver/cellulose acetate composite fibers, and silver nylon dressings were all proved to be antibacterial.[9,10] Beside an antibiotic ability, however, the principal function of a wound dressing is to provide an optimal healing environment, e.g., isolation from the external environment, complete coverage of the wound surface to prevent further contamination or infection, and maintenance of a moist microenvironment next to the wound surface.[11] Hydrogels consist of three-dimensional hydrophilic polymer networks in which a large amount of water is interposed. Because of their unique properties, a wide range of medical, pharmaceutical, and prosthetic applications have been proposed for them.[12] So hydrogel wound dressings are better choice than fabrics or films for burn injury treatment. Many polymers can be used to prepare hydrogels, such as poly(vinyl alcohol) (PVA) and poly(vinyl pyrrolidone) (PVP). PVA is a well-known biologically friendly polymer and has been developed for biomedical applications such as artificial pancreas,[13–15] synthetic vitreous body,[16] wound dressing, artificial skin, and cardiovascular device.[17,18] PVP is one of the most widely used polymers in medicine because of its solubility in water and its extremely low cytotoxicity.[19] A recent work described the topical application of PVP onto the skin for transdermal delivery of drugs.[20] Combination of the properties of PVA and PVP in PVA–PVP blends has led to the preparation of new biomaterials.[21,22] In our previous study,[23] physically crosslinked PVA–PVP hydrogels with perfect mechanical properties were prepared by cyclic freezing–thawing treatment.

In this paper, therefore, great attempts are made to incorporate silver nanoparticles into PVA–PVP hydrogels to combine the good mechanical strength of

Correspondence to: X. Jing (xbjing@ciac.jl.cn).
Contract grant sponsor: National Natural Science Foundation of China; contract grant numbers: 20274048, 50373043.
Contract grant sponsor: Chinese Academy of Sciences; contract grant number: KJCX2-SW-H07.

PVA–PVP hydrogel wound dressing and the powerful antibacterial ability of nanosilver together. The formulation and properties of this novel wound dressing, the *in vitro* release profiles of the silver ions from the hydrogel and the antibacterial activity against Gram-negative *Escherichia coli* (*E. coli*) and Gram-positive *Staphylococcus aureus* (*S. aureus*) are reported.

EXPERIMENTAL

Materials

Polyvinal alcohol (PVA) with a hydrolysis degree of 99.0–99.8% (molecular weight = 7.3×10^4–7.7×10^4) was supplied by Shanghai Chemical Reagent Company (Shanghai, China). PVP (molecular weight = 3.6×10^5) was purchased from BASF Chemical Co. (Ludwigshafen, Germany). These polymers were used without further purification. Silver nitrate ($AgNO_3$), sodium citrate and all other reagents were of analytical grade and used without further purification. Distilled water was used as solvent in all experiments.

Preparations

Preparation of silver sols

The silver nanoparticles were prepared by sodium citrate reduction of $AgNO_3$.[24] Typically, 18 mg of $AgNO_3$ was dissolved in 100 mL of distilled water and brought to boiling. Two milliliters of 1% solution of trisodium citrate was added, and the solution was kept on boiling for $\sim$ 1 h. The Ag sol prepared was greenish yellow.

Preparation of Ag/PVA–PVP composite hydrogels

A PVA–PVP aqueous solution was added into the prepared Ag sol. The total concentration of PVA and PVP was $\sim$ 12 wt % and the PVA-to-PVP weight ratio was 70 : 30. The weight contents of silver with respect to the PVA–PVP amount used were 0.1, 0.2, 0.4, 0.8, and 1.0 wt %, respectively. The mixture solution was put into the wells of a 24-well plate and was frozen at (-20°C for 12 h and then thawed at 25°C for 12 h. This treatment was repeated for three times and hydrogel disks of about 3 mm in thickness were obtained. The total solid content in the hydrogels was 12 wt %.

Preparation of Ag/PVA–PVP composite films

To investigate the interaction between silver and PVA–PVP matrix, nanosilver/PVA–PVP composite films were prepared as models for Ag/PVA–PVP hydrogels. The mixture solutions were prepared by the same method as for Ag/PVA–PVP hydrogels but the total concentration of PVA and PVP was $\sim$ 1 wt %. Then the mixture solutions were cast onto glass slides and dried in vacuum for 24 h at 60°C to obtain the composite films of ca.100 μm in thickness.

Characterization

Structure and morphology

UV–Vis spectra of the silver sols and the Ag/PVA–PVP films were collected using a UV-2400 spectrophotometer (2100, Shimadzu, Kyoto, Japan) with a slit width of 2.0 nm. The size distribution of the silver nanoparticles was measured using a transmission electron microscope (TEM-2010′TOEL, Tokyo, Japan) and a dynamic light scattering instrument (DLS) with a vertically polarized He–Ne laser (DAWN EOS, Wyatt Technology, Santa Barbara, CA) at a fixed scattering angle of 90° and at a constant temperature of 25°C. The structures of the Ag/PVA–PVP films were characterized by Fourier transform infrared spectroscopy (FTIR, Bruker Vertex 70, Ettlingen, Germany). A differential scanning calorimeter (DSC-7, Perkin–Elmer, Norwalk, CT) was employed to detect the crystalline status in the nanoAg/PVA–PVP films over the temperature range of 50–240°C at a scanning rate of 10°C/min under nitrogen protection. The surface and cross section morphology of the freeze-dried nanoAg/PVA–PVP hydrogels was examined using a field emission scanning electron microscope (FE-SEM, FEI/Philips, Hillsboro, OR).

Water take-up

The prepared hydrogel plates were immersed in distilled water of 200-folds mass at 37°C for 24 h,[23] then they were taken out and weighed after removal of the free water on the surfaces with filter paper. The equilibrium swelling-ratio (ESR) was calculated by

$$\mathrm{ESR}\ (\%) = (W_e - W_d)/W_d \times 100\%$$

where W_e was the weight of the swollen gel in equilibrium state and W_d was the solid weight in the hydrogel.

Release of silver ions from the hydrogels

The *in vitro* release profiles of silver ions from the hydrogels were obtained by the method developed by Radhesh Kumar.[25] Briefly, the hydrogels of 0.3 g was stored in a flask containing 10 mL aqueous medium (9.5 mL distilled water + 0.5 mL 0.1*N* HNO_3) at 37°C and the flask was oscillated at a frequency of

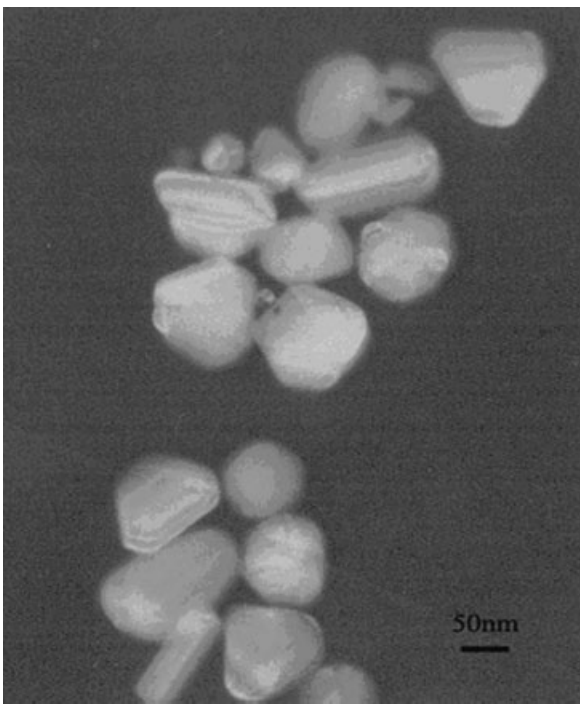

Figure 1 Typical TEM micrograph of the silver nanoparticles prepared by sodium citrate reduction of $AgNO_3$.

60 rpm in a rotary shaker. HNO_3 was added to protect the released Ag^+ ions from being reduced to metallic silver. The concentrations of silver ions released from the hydrogels into the water were measured using an inductively coupled plasma atomic absorbance spectrometer (SPS-1500 VR, Seiko Instruments, Tokyo, Japan).

Antibacterial ability of the nanoAg/PVA–PVP hydrogels

Antibacterial test was performed by modified Kirby Bauer technique and LB broth method.[26] Following two microorganisms were used: *S. aureus* strain 209, ATCC 25,923, which is Gram-positive and can exist on the body surface of mammals; *E. coli*, ATCC 25,922, which is Gram-negative and is a widespread intestinal parasite of mammals. The bacteria were cultivated at 37°C in sterilized LB broth (peptone 10 g, yeast extract 5 g, $NaNO_3$ 10 g, distilled water 1000 mL) at 90 rpm in a rotary shaker for 16 h. In the modified Kirby Bauer method, a droplet of 50 μL bacteria medium was dispensed onto an agar plate, then the hydrogel disks were placed and the incubation was continued for 24 h at 37°C. In the LB broth method, the hydrogel disks of 0.3 g were put in the flasks, which contained 10 mL aqueous medium at 37°C and were oscillated at a frequency of 60 rpm for periods ranging from 1 to 96 h. Then 3.0 mL of the above aqueous solution was mixed with 3.0 mL of the bacteria medium, the incubation was continued for another 6 h. Culture with pure LB broth served as control. The optical density (OD) of the bacterial broth medium at 600 nm was measured by a UV–vis spectrophotometer. The inhibition ratios for the nanoAg/PVA–PVP hydrogels were calculated as follows:

$$\text{Inhibition ratio } (\%) = 100 - 100 \times (A_t - A_0)/(A_{\text{con}} - A_0)$$

where A_0 was the OD for bacterial broth medium before incubation; A_t and A_{con} were the ODs for hydrogel and control sample after 6 h incubation, respectively.

RESULTS AND DISCUSSION

Silver nanoparticles

The silver nanoparticles were prepared as a nanosilver sol or a silver colloid by reducing $AgNO_3$ with sodium citrate. Their TEM image is shown in Figure 1. Their average size is about 100 nm. Their surfaces are smooth. Figure 2 shows their diameter distribution determined by DLS, ranging over 30–170 nm with an average of 100 nm. A typical absorption spectrum of the silver colloidal solution is shown in Figure 3(a). According to Ref. 27, this band is assigned to the surface plasmon absorption (SPR) of the nanosilver particles. It peaks at 425 nm and has a band width at half maximum of $\sim$ 130 nm, which is an indication of the particle size distribution.

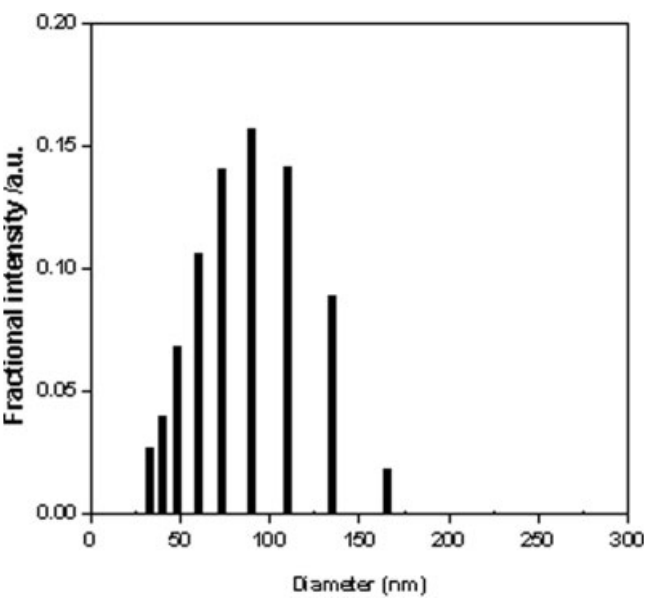

Figure 2 Size distribution of the silver nanoparticles determined by DLS measurement.

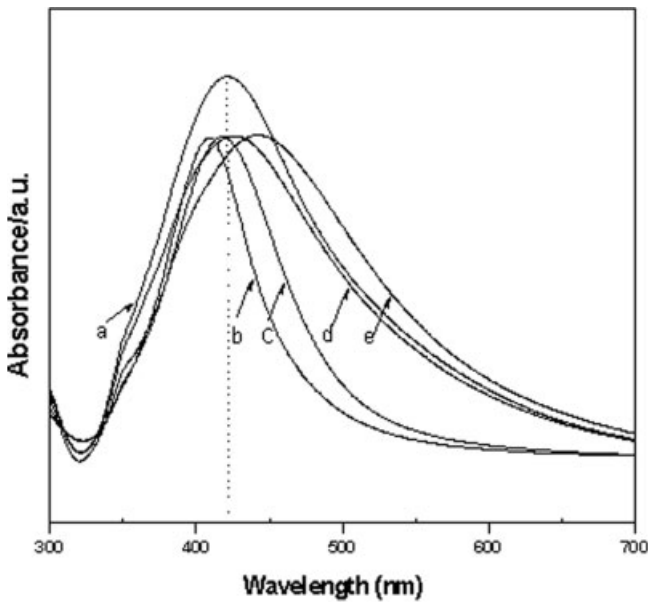

Figure 3 UV–vis absorption spectra of as-prepared silver sol in water (a) and nanoAg/PVA–PVP composite films (b–e). Silver contents: (b) 0.2 wt %; (c) 0.4 wt %; (d) 0.8 wt %; (e) 1.0 wt %.

Ag/PVA–PVP composite films

To investigate possible interactions between the silver nanoparticles and the PVA–PVP matrix in the Ag/PVA–PVP composite hydrogels and to understand the influence of the silver nanoparticles on the structure and performance of the hydrogels, composite, Ag/PVA–PVP films were prepared in the present study as a model of Ag/PVA–PVP hydrogels. The same mixture solutions were used for both composite films and composite hydrogels. Therefore, the model films have the same solid composition as the composite hydrogels. Because there is no interference of water in the model films, they can be easily characterized by various techniques.

Figure 3 also shows the UV–vis spectra of the Ag/PVA–PVP composite films. The SPR bands of the Ag/PVA–PVP composite films show different peak positions and peak widths. For the films containing 0.2, 0.4, 0.8, and 1.0 wt % of nanosilver, the bands peak at 410, 419, 425, and 443 nm, respectively. Compared with Figure 3(a) for the pure silver colloidal solution, the first two show blue-shifts while the other two show red-shifts. Among the four composite films, only the one containing 1.0 wt % of silver shows comparable band width (160 nm) to the colloidal solution, the rest three give narrower band widths (70–130 nm). It has been proved that PVA and PVP are both good stabilizing agents for silver nanoparticles.[27,28] So the blue-shifts and the narrower widths of the SPR bands can be explained as the smaller size and more uniform size distribution of the silver nanoparticles in the first two composite films and the red-shifts and wider width indicate the opposite variations, which can be induced by agglomeration of the Ag nanoparticles and/or change of the dielectric properties of the surrounding environment.[29] This can be further explained by considering the interactions between the nanosilver and the PVA–PVP matrix in the following discussions.

As seen in Figure 4, an increase of the silver content in the Ag/PVA–PVP composite films leads to enhancement of the 1145 cm^{-1} band for the films containing 0.1 and 0.2 wt % of nanosilver and to weakening of the same band for the films containing more nanosilver. This band can be assigned to C—O stretching vibration of PVA. It is a measure of the interaction between PVP and PVA. Its enhancement and weakening with silver-content reveal involvement of the nanosilver in the interaction between PVP and PVA.

The DSC traces of pure PVA–PVP and nanoAg/PVA–PVP composite films with various contents of silver are shown in Figure 5. The melting temperatures (T_m), glass transition temperatures (T_g) and melting enthalpies (ΔH_m) of the various samples are listed in Table I. Sure enough, the T_m, T_g, and ΔH_m all show similar variations with increasing nanosilver content, i.e., increasing (T_g and ΔH_m) or decreasing (T_m) for the films containing 0.1, 0.2 and 0.4 wt % of nanosilver and changing reversely for those films containing more nanosilver. It is noticed that all Ag/PVA–PVP films show more ΔH_m than the PVA–PVP film. These results differ from that reported by Z. H. Mbhele et al.[29] In their study, incorporation of silver particles, with average diameter of 5 nm, into the PVA matrix led to a dramatic decrease in T_m and increase in

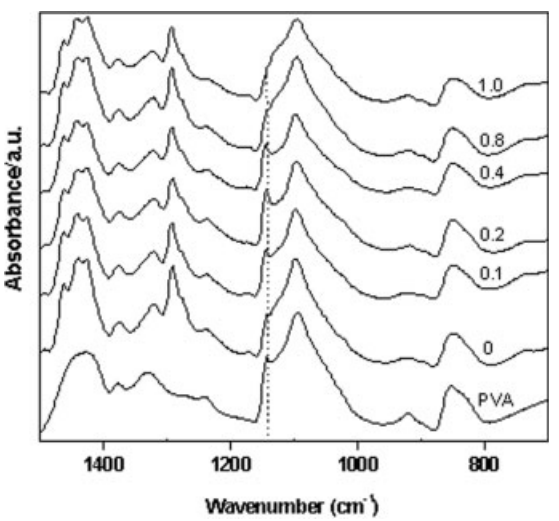

Figure 4 FTIR spectra of pure PVA–PVP and nanoAg/PVA–PVP composite films with different Ag contents (0.1, 0.2, 0.4, 0.8, and 1.0 wt %).

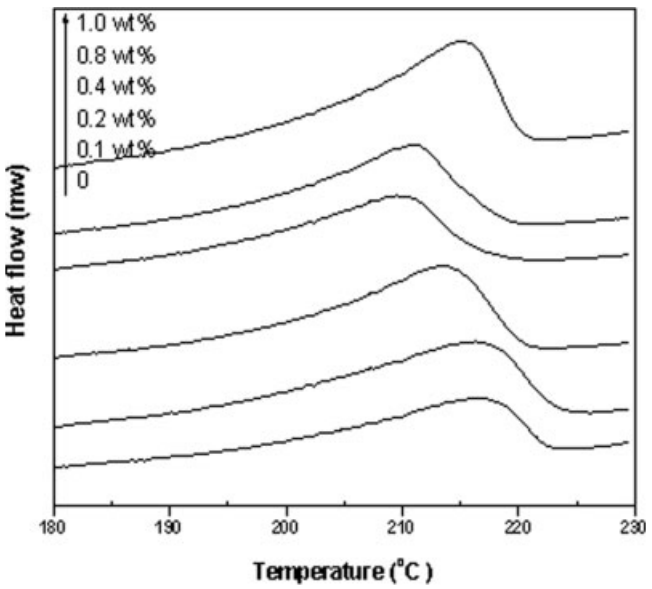

Figure 5 DSC curves of pure PVA–PVP and nanoAg/PVA–PVP composite films with various contents of silver (For clarity, curves are presented in the range 180–230°C. Heating rate 10°C/min).

T_g both by more than 20°C but did not affect crystallinity in PVA. They explained the observed effects as the reduced mobility of the PVA chains attached to the surface of the Ag nanoparticles. To explain the above results of UV–vis, FTIR, and DSC observations, we have to consider the possible interactions in the Ag/PVA–PVP systems, i.e., those between PVA and PVP, between PVA and nanosilver, and between PVP and nanosilver. In the previous work,[23] we proved that the crystallinity of PVA in PVA–PVP hydrogels decreased with increasing PVP content, because of the interference of PVP to the crystallization of PVA. It seems that the PVP has stronger interaction than the PVA does with the silver particles. When silver particles are added into the PVA–PVP matrix, they interact with the PVP molecules preferentially, the interaction between PVA and PVP molecules is weakened, which results in the improvement of the crystallinity of PVA in the composite (indicated by the increase of ΔH_m). On the other hand, interactions between the silver particles

TABLE I
Melting Enthalpy (ΔH_m), Melting Peak Temperature (T_m), and Glass Transition Temperature (T_g) of Pure PVA–PVP and Ag/PVA–PVP Composite Films

Ag (wt %)	T_g (°C)	T_m (°C)	ΔH_m (J/g)
0	88.3	216.4	25.5
0.1	88.7	215.4	31.6
0.2	90.6	213	33.1
0.4	95	208.9	28.3
0.8	87.1	210.4	32
1	88.6	214.7	34

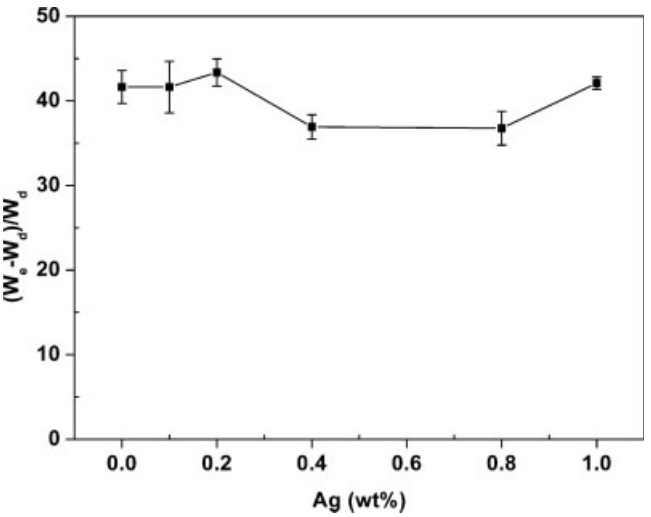

Figure 6 Water absorption ability of pure PVA–PVP and nanoAg/PVA–PVP composite hydrogels with various contents of silver.

and the PVA molecules still exist, so mobility of the PVA chains attached to the surfaces of the Ag particles is reduced.[29] When silver content is 0.4 wt %, the lowest T_m and highest T_g are obtained. Further increment of the silver content results in aggregation of the silver nanoparticles, weakening of their interactions with both PVA and PVP, and enhancement of the interaction between PVP and PVA. This is in accordance with the FTIR data.

On the basis of the above results, we can draw a conclusion that silver particles could be equably dispersed in the PVA–PVP hydrogel matrix due to their interaction with the PVA–PVP matrix. Therefore, PVA–PVP hydrogel could be used as an eligible silver nanoparticle carrier to prepare silver-containing hydrogels used for wound dressing.

Ag/PVA–PVP composite hydrogels

Water absorption

Besides good mechanical properties, a hydrogel wound dressing has to absorb the exudates on the wound surface and provide a wet environment for the wound. So the water absorbing and keeping ability of hydorgels is very important. Water-take-up ability of the Ag/PVA–PVP hydrogels is shown in Figure 6. It can be found that all hydrogels show a swelling ratio as high as 40 folds, which is enough for hydrogel wound dressings. The incorporation of the nanosilver in the hydrogel does not influence the water absorption ability.

SEM analysis

It is well known that a porous surface is important for the transport of oxygen from outside to inside of

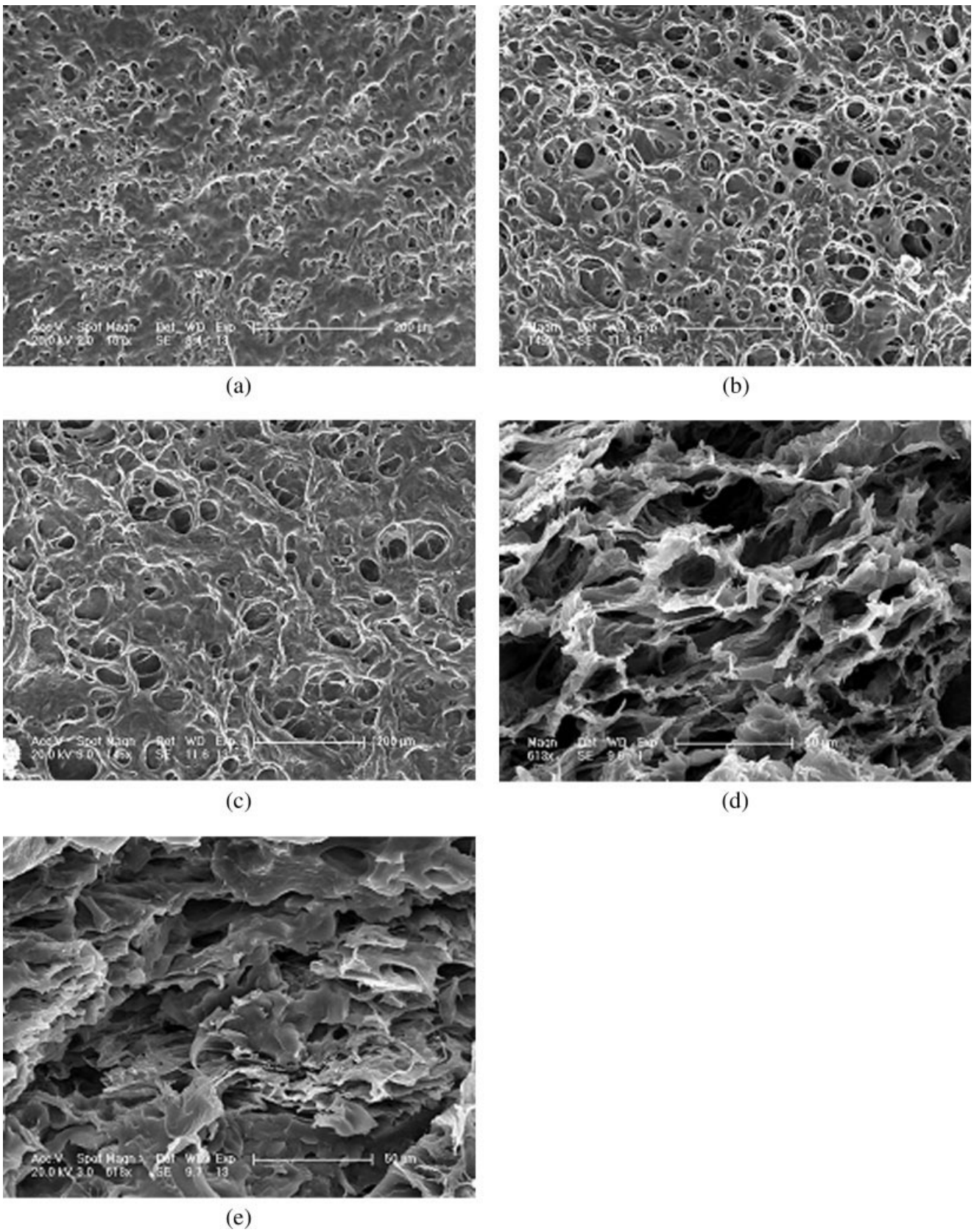

Figure 7 SEM images of pure PVA–PVP and nanoAg/PVA–PVP composite hydrogels. (a) surface image of PVA–PVP hydrogel plate; (b) surface image of 0.1 wt % Ag/PVA–PVP hydrogel plate; (c) surface image of 0.8 wt % Ag/PVA–PVP hydrogel plate; (d) cross-section image of 0.1 wt % Ag/PVA–PVP hydrogel plate; (e) cross-section image of 0.8 wt % Ag/PVA–PVP hydrogel plate.

the wound dressing, and a three-dimensional network structure is crucial to absorbing and keeping large amount of water in hydrogel materials. We examined the surface and cross-sectional morphologies of Ag/PVA–PVP composite hydrogels by SEM. As shown in Figure 7, porous surface morphology and three-dimensional network structure in the cross section are formed in both PVA–PVP and Ag/PVA–PVP hydrogels. No distinguished difference is found for the hydrogels with different silver contents. No serious aggregation of the nanoparticles is observed even when the silver content is up to 1 wt %. This can be explained as a stable network structure formed in the hydrogels and the strong interaction between the silver particles and the PVA and PVP molecules as we have discussed in the previous section.

In vitro release of silver ions from the hydrogels

The antimicrobial activity of silver is dependent on the silver cation Ag^+, which binds strongly to electron-donating groups in biological molecules containing sulfur, oxygen or nitrogen. Hence the silver-based antimicrobial polymers have to release the Ag^+ to a pathogenic environment to be effective. In this work the silver release model developed by Radhesh Kumar was employed, and atomic absorption spectroscopy (AAS) was used for the quantitative determination of the silver ion released from the hydrogels.[25] Five Ag/PVA–PVP hydrogel samples with silver contents of 0.1, 0.2, 0.4, 0.8, and 1.0 wt % with respect to total PVA–PVP weight were used. The duration of 96 h was selected for the release experiment to study the whole release process of the silver ions. As shown in Figure 8(A), the release of silver ions from the hydrogels is very quick at the beginning and then became slower and slower. The silver ion release shows dependence to some extent on the silver content in the hydrogels. For example, the amount of silver ions released in the first 12 h increases with increasing silver content in the hydrogels, being 0.20, 0.45, 1.35, 3.76, and 6.26 ppm for the samples containing 0.1, 0.2, 0.4, 0.8, and 1.0 wt % of silver content, respectively. When the silver ion concentration released is plotted against square root of incubation time $h^{1/2}$ [Fig. 8(B)], linear relationships are obtained, except for the initial stages of soaking. This indicates that the release of silver ions is controlled by the interdiffusion of the ions within the hydrogel.[30]

In vitro antibacterial effect

Using a modified Kirby Bauer technique, the bactericidal effects of two Ag/PVA–PVP hydrogels and pure PVA–PVP hydrogel were evaluated comparatively.[26] After 24 h incubation at 37°C, the Ag/PVA–PVP hydrogels showed antibacterial effect on Gram-positive *S. aureus* and Gram-negative *E.coli*. The diameter of inhibition zone for the 1.0 wt % Ag/PVA–PVP hydrogel is slightly larger than that for the 0.2 wt % Ag/PVA–PVP sample (see Fig. 9). As a control, the pure PVA–PVP hydrogel showed no inhibition ability. Elemental silver has been believed to function antimicrobially either as a release system for silver ions or as a contact-active material.[31] In the present study, the Ag/PVA–PVP hydrogels seem to be only contact-active. The diffusing ability of the silver ions on agar plate might have been limited by the formation of secondary silver compounds, which is the limitation of the Kirby Bauer technique as a quantitative tool to determine the antimicrobial activity.[32] Therefore, LB medium method was intro-

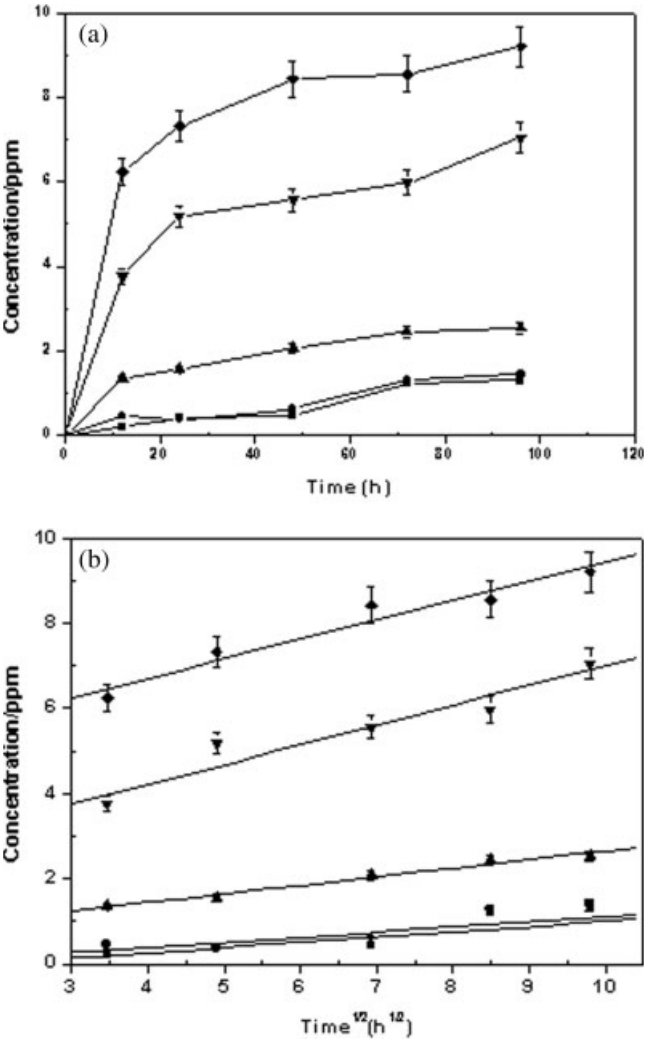

Figure 8 Silver ion release profiles of nanoAg/PVA–PVP composite hydrogels with various contents of silver: (A) the concentration of silver ion released versus time; (B) the concentration of silver ion released versus square root of time. (□)1.0 wt %; (▼) 0.8 wt %; (▲) 0.4 wt %; (●) 0.2 wt %; (■) 0.1 wt %.

duced to determine the antimicrobial activity of Ag/PVA–PVP hydrogels quantitatively.[26] Pure PVA–PVP hydrogel and four Ag/PVA–PVP samples (Ag wt % = 0.1, 0.2, 0.4, and 1.0, respectively) were tested. As shown in Figure 10, the antibiotic ability to *E.coli*, expressed as inhibition ratio, was enhanced with increasing silver content in the hydrogels. When the silver content was 1.0 wt %, the inhibition ratio reached up to 90%.

CONCLUSIONS

The PVA–PVP hydrogels containing silver nanoparticles were prepared through repeated freezing–thawing treatment. The silver content with respect to the polymers used was in the range of 0.1–1.0 wt %. The silver particle size was from 20 to 100 nm as measured by TEM and SDLS. By using PVA–PVP films containing silver particles as a model, the influence of silver nanoparticles on the properties of PVA–PVP matrix was investigated by UV–vis, DSC, and FTIR, the morphology of freeze-dried PVA–PVP hydrogel matrix and dispersion of the silver nanoparticles in the matrix was examined by SEM. It was found that a three-dimensional structure was formed during the process of freezing–thawing treatment and no serious aggregation of the silver nanoparticles occurred. Water absorption properties, the release of silver ions from the hydrogels were investigated, and the antibacterial effects of the hydrogels against *E. coli* and *S. aureus* were examined by modified KB method and LB broth method. It was proved that the nanosilver-containing hydrogels had an excellent antibacterial performance.

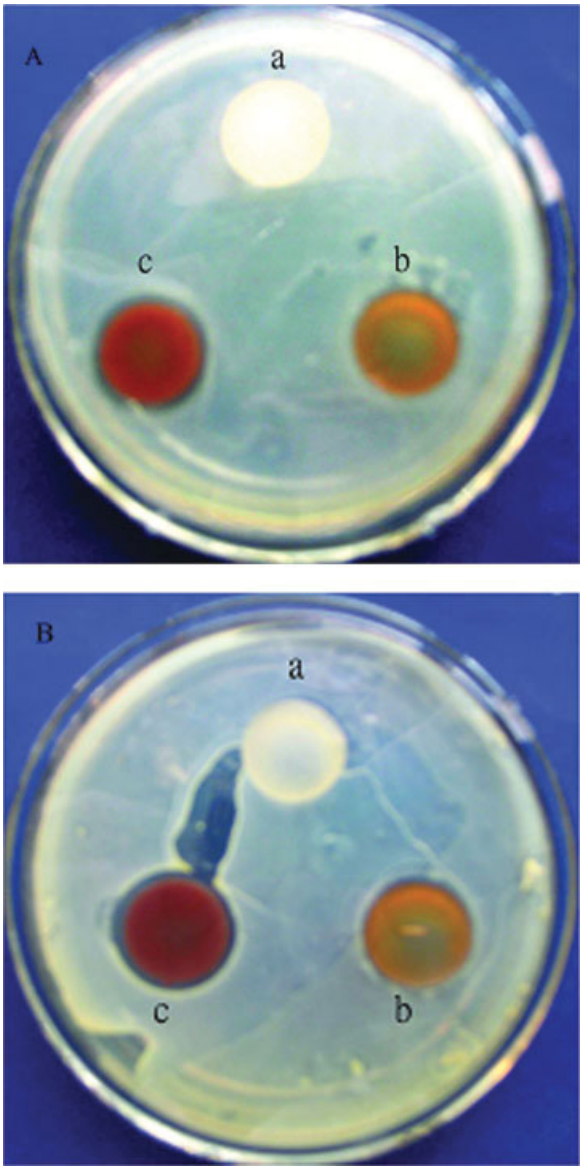

Figure 9 Antibacterial test results for *E. coli* (A) and *S. aureus* (B) after 24 h incubation. (a) PVA–PVP hydrogel; (b) 0.2 wt % Ag/PVA–PVP hydrogel; (c) 1.0 wt % Ag/PVA–PVP hydrogel. [Color figure can be viewed in the online issue, which is available at www.interscience.wiley.com.]

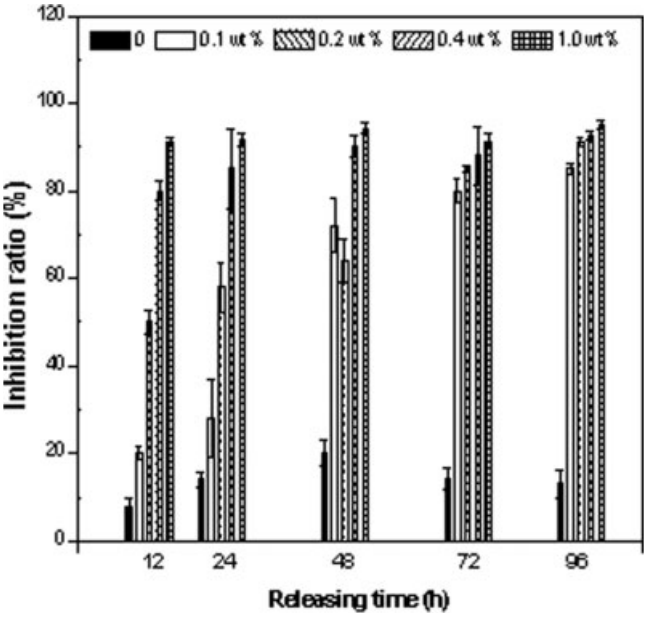

Figure 10 Quantitative evaluation of *in vitro* inhibition ability to *E. coli* of the pure PVA–PVP and Ag/PVA–PVP hydrogels in 6 h duration.

We thank Professor Shan Chen of Northeast Normal University in China for providing the microorganisms *S. aureus* and *E. coli*.

References

1. Greenfield, E.; McManus, A. T. Nurs Clin North Am 1997, 32, 297.
2. Klasen, H. J Burns 2000, 26, 117.
3. Klasen, H. J Burns 2000, 26, 131.
4. Tsipouras, N.; Rix, C. J.; Brady, P. H. Clin Chem 1997, 43, 290.
5. Mi, F. L.; Wu, Y. B.; Shyu, S. S.; Schoung, J. Y.; Huang, Y. B.; Tsai, Y. H.; Hao, J. Y. J Biomed Mater Res 2002, 59, 438.

6. Yu, S. H.; Mi, F. L.; Wu, Y. B.; Peng, C. K.; Shyu, S. S.; Huang, R. N. J. Appl Polym Sci 2005, 98, 538.
7. Mi, F. L.; Wu, Y. B.; Shyu, S. S.; Chao, A. C.; Lai, J. Y.; Su, C. C. J Membrane Sci 2003, 212, 237.
8. Son, W. K.; Youk, J. H.; Lee, T. S.; Park, W. H. Macromol Rapid Commun 2004, 25, 1632.
9. Balogh, L.; Swanson, D. R.; Tomalia, D. A.; Hagnauer, G. L.; McManus, A. T. Nano Lett 2001, 1, 18.
10. Vuong, T. E.; Franco, E.; Lehnert, S.; Lambert, C.; Portelance, L.; Nasr, E.; Faria, S.; Hay, J.; Larsson, S.; Shenouda, G.; Souhami, L.; Wong, F.; Freeman, C. Int J Radiat Oncology Biol Phys 2004, 59, 809.
11. Nho, Y. C.; Park, K. R. J Appl Polym Sci 2002, 85, 1787.
12. Drury, J. L.; Mooney, D. J. Biomaterials 2003, 24, 4337.
13. Giusti, P.; Lazzeri, L.; Barbani, N. J Mater Sci Mater Med 1993, 4, 538.
14. Young, T. H.; Yao, N. K.; Chang, R. F.; Chen, L. W. Biomaterials 1996, 17, 2139.
15. Young, T. H.; Chuang, W. Y.; Yao, N. K.; Chen, L. W. J. Biomed Mater Res 1998, 40, 385.
16. Inoue, K.; Fujisato, T.; Gu, Y. J.; Burczak, K.; Sumi, S.; Kogire, M.; Tobe, T.; Uchida, K.; Nakai, I.; Maetani, S.; Ikada, Y. Pancreas 1992, 7, 562.
17. Burczak, K.; Gamian, E.; Kochman, A. Biomaterials 1996, 17, 2351.
18. Rosiak, J. M.; Ulanski, P. Radiat Phys Chem 1999, 55, 139.
19. Razzak, M. T.; Zainuddin, E.; Dewi, S.; Lely, H.; Taty, S. Radiat Phys Chem 1999, 55, 153.
20. Lopes, C. M. A.; Felisberti, M. I. Biomaterials 2003, 24, 1279.
21. Cassu, S. N.; Felisberti, M. I. Polymer 1997, 38, 3907.
22. Seabra, A. B.; Oliveira, M. G. Biomaterials 2004, 25, 3773.
23. Yu, H. J.; Xu, X. Y.; Chen, X. S.; Hao, J. Q.; Jing, X. B. J. Appl Polym Sci accepted.
24. Jin, Y. D.; Dong, S. J. J Phys Chem B 107: 12902 2003.
25. Kumar, R.; Unstedt, H. M. Biomaterials 2081 2005, 26.
26. Melaiye, A.; Sun, Z. H.; Hindi, K.; Milsted, A.; Ely, D.; Reneker, D. H.; Tessier, C. A.; Youngs, W. J. J Am Chem Soc 2005, 127, 2285.
27. Yin, B. S.; Ma, H. Y.; Wang, S. Y.; Chen, S. H. J Phys Chem B 107: 8898 2003.
28. Gaddy, G. A.; Korchev, A. S.; McLain, J. L.; Slaten, B. L.; Steigerwalt, E. S.; Mills, G. J Phys Chem B 2004, 108, 14850.
29. Mbhele, Z. H.; Salemane, M. G.; Sittert, C. G. C. E.; Nedeljkovicć, J. M.; Djoković, V.; Luyt, A. S Chem Mater 2003, 15, 5019.
30. Kawashita, M.; Toda, S.; Kim, H. M.; Kokubo, T.; Masuda, N. J Biomed Mater Res 2003, 66, 266.
31. Chan, H. H.; Jan, T.; Christina, S.; Ralf, T.; Joerg, C. T. Advanced Materials 2004, 16, 967.
32. Nomiya, K.; Tsuda, K.; Sudoh, T.; Oda, M. J Inorg Biochem 1997, 68, 39.